FE^2 Multiscale Modelling of Chloride Ions transport in Recycled Aggregates Concrete

A. FANARA, L. COURARD & F. COLLIN
Urban and Environmental Engineering, University of Liège, Liège, Belgium.

ABSTRACT: In the context of climate change, reducing the production of CO_2 emissions and preserving natural resources have proven to be necessary. One way to reach theses objectives is to recycle old concrete members: Recycle Concrete Aggregates (RCA) are aggregates obtained by crushing demolished concrete structures. Those aggregates can substitute the Natural Aggregates (NA) inside the so-called Recycled Aggregates Concrete (RAC). RCA are composed of natural aggregates and adherent mortar paste, the latter increasing the porosity and water absorption of RAC. Furthermore, water is necessary for, and even promotes, the penetration of aggressive ions such as chloride ions, possibly reducing the durability of said concrete.
This paper aims to model the influence of RCA on chloride ions ingress: several experiments have been performed to determine the transfer properties and the chloride ions diffusion coefficients of mortar pastes and concretes produced with NA or 100% RCA. The microstructure of the RCA deeply influences the permeability, the water content distribution and the chloride diffusion. These properties have been included into a numerical model that integrates the microstructural information. A numerical homogenization technique, based on the Finite Element square (FE^2) method, is implemented into a coupled multiscale model of water flows and advection/diffusion of chlorides in saturated concrete, in order to model the complex flow behaviour encountered.
The numerical model developed is compared to existing simple-scale models, using a simple RVE, in order to validate the implementation. The numerical convergence of the developed model is also studied, as far as the numerical cost of the FE square method is expensive.

1 INTRODUCTION

Maintenance and rehabilitation of concrete structures represent a significant and continuously increasing cost. In the vicinity of roads (where de-icing salts are used in winter) and coastal areas, the major cause of degradation of reinforced concrete structures is chloride attacks (Mangat & Molloy 1994)(Morga & Marano 2015). Chloride ions leach into the concrete's porous system, reaching the steel rebars where they eventually concentrate. This leads to pitting and loss of section of the reinforcements, decreasing their strength and possibly leading to a structural failure (Angst, Elsener, Larsen, & Vennesland 2009). On the other hand, waste from the construction and demolition sector (C&D Waste) is one of the heaviest and most voluminous waste streams generated (European Commission 2019)(Zhao, Courard, Groslambert, Jehin, Léonard, & Xiao 2020). One popular way to reduce the amount of C&DW to be landfilled and simultaneously provide a sustainable source of aggregates for future building materials production is recycling. Recycled Concrete Aggregates (RCA) produced from crushed C&DW as a replacement of Natural Aggregates (NA) is one way to recycle, which has made it a thoroughly studied field of research (Hussain, Levacher, Quenec'h, Bennabi, & Bouvet 2000)(Nagataki, Gokce, Saeki, & Hisada 2004)(Belin, Habert, Thiery, & Roussel 2014). RCA are coarse particles containing both natural aggregates and residual adherent mortar paste, the latter impairing negatively their properties compared to NA: due to their increased porosity and water absorption, they favour the penetration of water and chloride ions, increasing the diffusivity of Recycled Aggregate Concrete (RAC) (Rao, Jha, & Misra 2007)(Akbarnezhad, Ong., Tam, & Zhang 2013)(Hu, Mao, Xia, Liu, Gao, Yang, & Liu 2018)(Sun, Chen, Xiao, & Liu 2020).

Concrete is a highly heterogeneous material due to its composition: its microstructure is composed of a wide range of components, from nanometre-sized pores to centimetre-sized aggregates (Garboczi & Bentz 1998). Modelling concrete and its entire microstructure is therefore computationally impossible,

and often the properties are homogenized over the entire microstructure to obtain mean values.
Nowadays, multiscale modelling and computational homogenization techniques allow to homogenize the concrete's microstructure over a certain scale, and then up-scale it while keeping the computational cost acceptable (Nilenius 2014). The multiscale modelling approach tends to combine the best of both the macroscopic approach and the microscopic approach (Bertrand, Buzzi, Bésuelle, & Collin 2020):

1. Macroscale: the concrete is treated as a homogeneous medium, and the constitutive laws are supposed to represent the whole behaviour of the material. The mixture theory allows to account for multiple phases (e.g. liquid water and water vapour) percolating inside the porous system of the material studied (Bear & Verruijt 1987). This method is easy to implement and allows the use of general properties of concrete, determined experimentally for example. Unfortunately, it means that each modification of the microstructure requires a new experimental campaign to obtain the homogenized properties of the material.

2. Microscale: the whole structure, including the heterogeneities (aggregates, porosity, ...) is directly represented in the model. Each microscopic constituent has its own constitutive equations. Although this increases the precision of the model, its computation cost is too high to be used on metre-sized structures.

The chloride ingress inside RAC being highly dependent on the microstructure of concrete, it is therefore necessary to use a multiscale model for that purpose.

Modelling the advection/diffusion of chloride in the water requires the replacement of the macroscopic phenomenological quantities of interest (e.g. flow measures, pore pressure or gradient of pore pressure) by suitable averages over this RVE. The constitutive equations (Darcy's and Fick's laws among others) are indeed applied only at the microscopic scale and homogenization/localization equations are employed to compute the macroscopic flows based on the pore pressure state at the microscopic scale. It has to be reminded that due to the separation of scale, the diffusion problem is solved under the assumption of steady-state at the microscale. Advective and diffusive transport modes and adsorption of chlorides are to be included in the model.

The homogenization technique used is considered as a numerical homogenization: it is called the unit cell method. This technique is based on the concept of representative volume element (RVE) (Kouznetsova, Brekelmans, & Baaijens 2001). The macroscopic phenomenological equations are replaced by averages over the RVE. The material properties and behaviour at the macroscale are therefore obtained from the modelling of this RVE, volume that contains a detailed model of the microstructure of the material (Kouznetsova, Brekelmans, & Baaijens 2001)(Bertrand, Buzzi, Bésuelle, & Collin 2020). In a sense, the RVE is meant to decouple the macrostructure from the microstructure in a computational way (Smit, Brekelmans, & Meijer 1998).

Using this method, the behaviour of the material and its properties are not valid for the whole macroscopic structure, but rather at some macroscopic points where an estimation is obtained through calculations on the RVE assigned to that macroscopic point (Kouznetsova, Brekelmans, & Baaijens 2001).
Each integration point of the discretized homogenized macrostructure is then linked to a RVE and finite element computations are performed separately for each RVE. The macroscopic pressure gradients and mean pressure are then transformed into boundary conditions applied to the RVE, and the macroscopic fluxes are computed by averaging the fluxes obtained for each RVE over their respective volume (Smit, Brekelmans, & Meijer 1998)(Kouznetsova, Brekelmans, & Baaijens 2001). This averaging is possible thanks to the periodicity of the microstructure in the vicinity of the integration point.
The method is called FE^2 method because the modelling is achieved by a finite element analysis on both the macroscale and microscale (RVE).

In this work, the microscale is referred to as the mesoscale as it consists of the scale of samples at the laboratory. The Representative Volume Element (RVE) therefore represents the structure of a concrete sample, that is a homogenized mortar paste (with homogenized properties, as for a macroscale solution) as well as impervious aggregates and adherent mortar paste. The ITZ between them could be accounted for through interface elements, but their influence would be difficult to quantify experimentally.
The macroscale, on the other hand, represents a metre-sized civil engineering structure.

At the mesoscale, the parameters used in the equations represent properties of a single phase among the two cited before when the integration point is in that phase. However, this means that for the mortar phase, which is a composite material, the properties used must be effective properties for the composite (Xi & Bazant 1999). At the macroscale, concrete is considered as a single phase composite material and all its properties are therefore averaged effective properties.

The material structure is assumed to be macroscopically homogeneous but microscopically het-

erogeneous. However, in concrete, the microscopic length scale is still bigger than at the molecular level, allowing the use of continuum mechanics as for the macroscale.

The FE^2 method is therefore a numerical double-scale method based on four consecutive and iterative steps performed on each Gauss point of the mesh until convergence of both scales (Bertrand, Buzzi, Bésuelle, & Collin 2020). For our application, those four steps could be described as follows:

1. From macroscale to mesoscale: the gradients and mean pressures of the macroscale are localised at the mesoscale through boundary conditions;
2. Resolution of the problem based on those boundary conditions at the mesoscale;
3. From mesoscale to macroscale: the fluxes of the mesoscale are homogenised into a unique flux for each Gauss point of the macroscale;
4. Resolution of the boundary value problem at the macroscale.

This iterative process is represented in the Figure 1. In the example of an application on an engineering structure, the macroscale would represent its mesh, where four elements are shown, each containing four Gauss points. The conditions applied to this structure (i.e. water pressure and pollutant concentration) and the gradients created by those are first localised in the mesoscale, represented by a slice of concrete multi-centimetres large. Then, based on those gradients and mean values, the boundary value problem is solved at the mesoscale and fluxes are deduced from it. However, all those fluxes must then be homogenised to obtain an unique value for the Gauss point studied. Then, once each Gauss point of each element used to mesh the engineering structure have a macroscopic flux assigned, the boundary value problem is solved at the macroscale.

2 METHODOLOGY

2.1 *General Multiscale Formulation*

The start of every multiscale formulation is the splitting of the scalar field ϕ in an additive manner, such that it contains both the macroscale part ϕ^M and the subscale part ϕ^f which contains the fluctuations of the total scalar field (Nilenius 2014)(Bertrand, Buzzi, Bésuelle, & Collin 2020):

$$\phi = \phi^M + \phi^f \tag{1}$$

On the boundaries Γ of the RVE, it is assumed that $\phi = \phi^M$ and therefore $\phi^f = 0$.

Following a Taylor expansion, limited to its first order inside the macroscale continuum, the homogenisation follows the assumption that ϕ^M varies linearly within the RVE, yielding the following equation:

$$\phi^M(x, \bar{x}) \approx \bar{\phi}(\bar{x}) + \bar{g}(\bar{x}) \times (x - \bar{x}) \quad \forall x \in \Omega \tag{2}$$

which is represented in the Figure 2 for a 1D RVE. In this formulation, $\bar{x}$ is the center of the RVE and $\bar{g}$ is a gradient defined such that:

$$\bar{g}(\bar{x}) = \text{grad}\ \bar{\phi}\ (\bar{x}) \tag{3}$$

In the subscale, the scalar field is not necessarily continuous and therefore, the higher order terms of the Taylor expansion cannot be neglected. They are then replaced by the fluctuation field, noted ϕ^f and resulting from the variations in the material properties of the RVE:

$$\begin{aligned}\phi(x, \bar{x}) &= \phi^M(x, \bar{x}) + \phi^f(\bar{x}) \\ &= \bar{\phi}(\bar{x}) + \bar{g}(\bar{x}) \times (x - \bar{x}) + \phi^f(\bar{x})\end{aligned} \tag{4}$$

As the equality between the macroscale-part and the subscale-part of the field is to be true for any point of the macroscale, it follows that:

$$\bar{g}(\bar{x}) \times (x - \bar{x}) + \phi^f(\bar{x}) \ll \bar{\phi}(\bar{x}) \tag{5}$$

which is the concept of separation of scales: the subscale characteristic length l_c^s must be negligible compared to the characteristic fluctuation length L_c^M of the macroscopic field:

$$l_c^s \ll L_c^M \tag{6}$$

If this assumption doesn't hold, then the boundary conditions of the subscale boundary value problem cannot be determined by the local macroscale pressure/concentration gradient, at least not under first-order homogenisation.

The transition from the subscale to the macroscale has an important characteristic that is the transfer of the flux. Indeed, in stationary conditions, the mass balance equation is:

$$\boldsymbol{\nabla} J = 0 \quad \text{in } \Omega \tag{7}$$

where J is the flux and Ω the domain where the material heterogeneities are embedded (i.e. the mesoscale). Splitting the scalar field as shown previously, in addition to first order homogenisation, allows to identify the volume average of the flux inside the RVE, that is the macroscale flux $\bar{J}$:

$$\bar{J} = \frac{1}{|\Omega|} \int_{\Omega} J(x)\, d\Omega \tag{8}$$

where Ω denotes the reference domain occupied by the RVE.

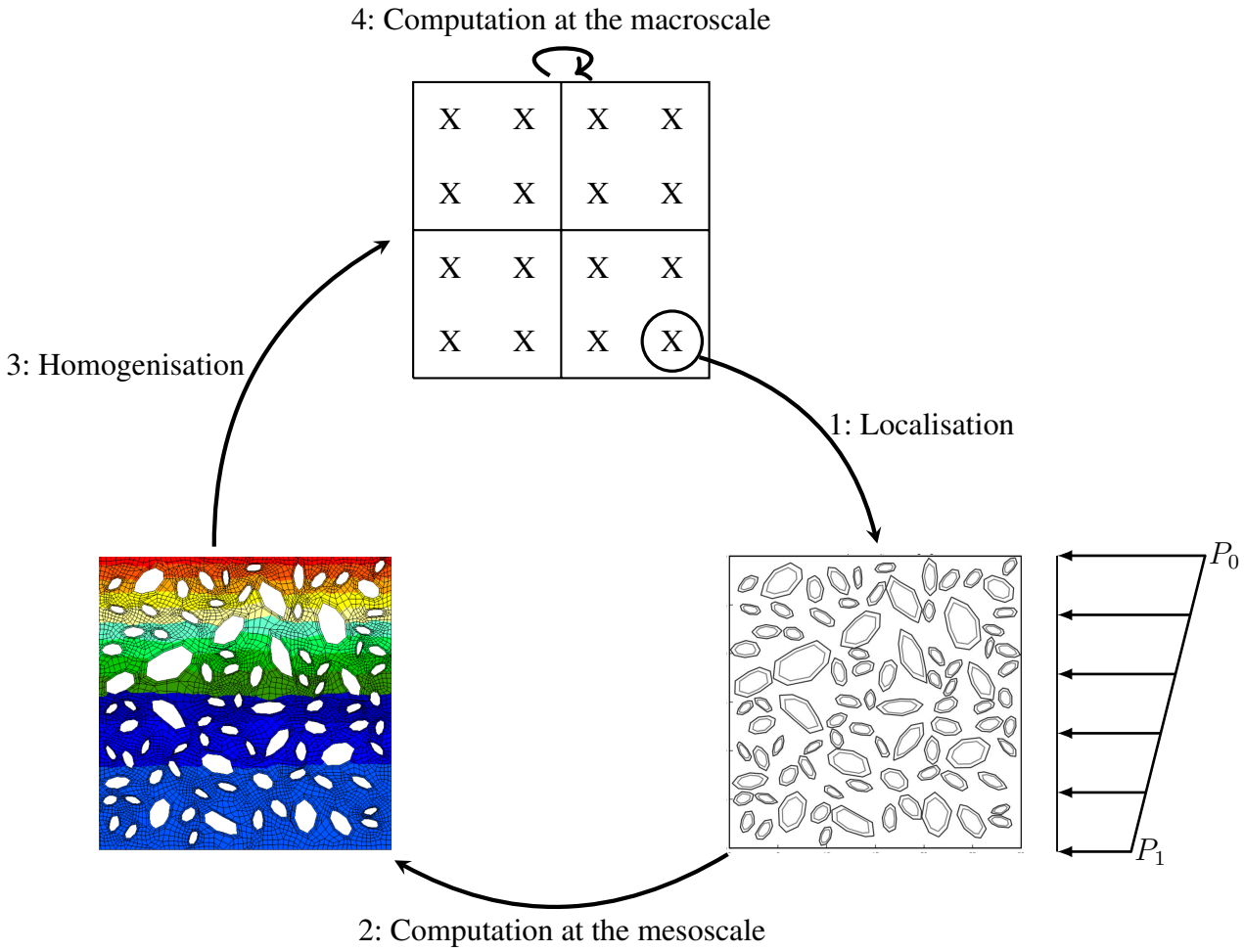

Figure 1: Representation of the iterative process performed on each Gauss point of the mesh during the multiscale computation.

2.2 *RVE Generation*

The first step to a multiscale FE^2 study is the generation of the RVE. The RVE is multiphasic: impervious natural aggregates are considered inside a porous mortar matrix. For the case of RCA, an additional mortar gangue is also considered, whose properties are different of the ones of the mortar matrix.

The RVE must be representative of the material studied, and it is therefore essential to use and respect properties related to the concrete: the surface fraction of aggregates, the aspect ratio and the particle size distribution of the aggregates are used in the generation. Each aggregate has a random size, position and orientation following the properties given above. Therefore, it is impossible to generate two times the same RVE.
Then, using an algorithm adapted from the one of Nilenius (Nilenius 2014), a 2D RVE is generated and meshed in 2D by the software GMSH (Geuzaine & Remacle 2009), according to the Frontal-Delaunay algorithm for quads, with a simple recombination algorithm applied to all surfaces, ensuring that all elements are quads.
The size of the RVE is dictated by the maximum aggregate diameter, so as to keep a size of at least 3 times that diameter. An example of a RVE with RCA of 8mm of maximum diameter is represented in the Figure 3.

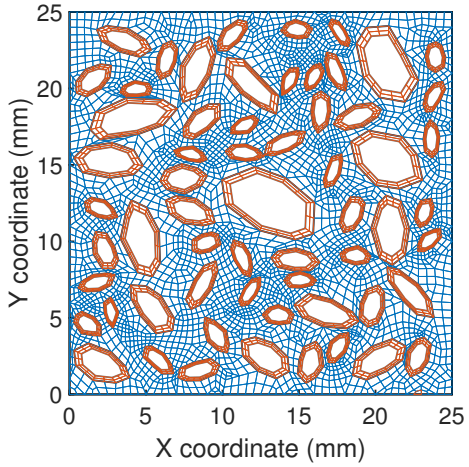

Figure 3: Example of an RVE generated for RAC.

One may see that the mesh is more refined around the aggregates. It is due to the octagonal form of the aggregates that requires many points and elements. Even though the sample is small, its complexity is therefore resulting in a high number of nodes and elements, which is not ideal for the multiscale modelling, but required for precision purposes.

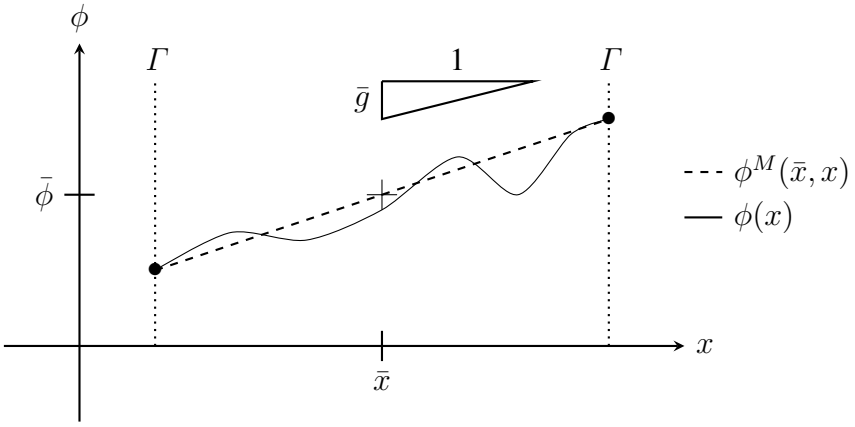

Figure 2: Illustration of the ϕ^M properties and its linear variations within a 1D RVE domain Ω (modified from Nilenius (2014, 2015)).

One of the assumptions of this method is that the volume fraction is directly changed into a surface fraction, which is inaccurate because the aggregates are not spherical and therefore, the transformation from a volume to a surface may modify the granulometric curve, which is not accounted for here.
Modelling concrete should be performed with a three dimensional model as it is highly heterogeneous and its 3D porous structure may create preferential path in all directions. However, it requires a greater computational power and the equations solving the problem are also harder to develop.
In this research, the two-dimensional approach is preferred, keeping in mind that other authors, such as (Nilenius 2014), have done the comparison between 2D and 3D, yielding diffusivity coefficients up to 40% higher in 3D than in 2D. This is easily explained by the restriction created in 2D where the flow is required to by-pass the aggregates in the plane, while in 3D, an out-of-plane solution is possible.
Those hypotheses could be corrected by direct modelling methods and inverse modelling: the modelling of the experiments done will allow to verify that the sample is correct and if not, a penalisation will be applied to correct it.

2.3 *Multiscale Ingress Modelling under Saturated Conditions*

The first development of the models are performed under saturated conditions. The boundary conditions, i.e. water pressure and pollutant concentration variations, are applied on the macroscale. Gradients are then computed for each Gauss point and transmitted to the mesoscale, as well as the average pressure/ concentration at that point. At the mesoscale, each integration point has an assigned value for the water pressure and pollutant concentration, based on the average pressure/concentration and theur respective gradients localized from the macroscale. Once those conditions are applied, the resolution can start.

2.3.1 *Mesoscale Water flows under saturated conditions*

The mass balance equation of water, in a fixed and undeformable system, under saturated conditions and under the assumption of steady-state, is:

$$\frac{\partial}{\partial x_i}\left(\rho_w \, v_i^w\right) = 0 \tag{9}$$

where ρ_w is the water density [kg/m^3] and v_i^w is the fluid flow rate per unit area [m/s].

The Equation 9 represents the mass variation of liquid water inside the porous matrix of concrete. The first factor of the equation, the water density, varies with the internal pressure of the matrix (noted $P_{w,average}$):

$$\rho_w = \rho_{w0} \times \left(1 + \frac{P_{w,average} - P_{w0}}{\chi_w}\right) \tag{10}$$

where ρ_{w0} [kg/m^3] and P_{w0} [Pa] are, respectively, the initial density of liquid water and the initial pressure inside the porous structure. This relation is dependent on the fluid compressibility, noted χ_w [Pa$^-$1] (at 20°C, $1/\chi_w = 5\ 10^{-10}$ Pa^{-1}).

The second factor of the Equation 9 is related to the liquid water convection. The Darcy's law is used to describe the movement of a fluid (water) inside a porous medium. Under the hypothesis of a homogeneously permeable medium, and in the absence of gravitational forces, the fluid flux is directly proportional to the gradient of pressure (noted ∇P_w):

$$v_i^w = -\frac{k}{\mu_w}\frac{\partial P_w}{\partial x_i} \tag{11}$$

where k [m^2] is the intrinsic permeability of the porous medium, and μ_w [kg/m.s] is the dynamic viscosity of the fluid.

The stifness matrix, under saturated conditions and for water flows only, is quite simple:

$$K = \begin{bmatrix} \frac{\partial \nabla(\rho_w\, v_1^w)}{\partial \nabla P_w} & \frac{\partial \nabla(\rho_w\, v_1^w)}{\partial P_w} \\ \frac{\partial \nabla(\rho_w\, v_2^w)}{\partial \nabla P_w} & \frac{\partial \nabla(\rho_w\, v_2^w)}{\partial P_w} \end{bmatrix} = \begin{bmatrix} \frac{k \times \rho_w}{\mu_w} & 0 \\ \frac{k \times \rho_w}{\mu_w} & 0 \end{bmatrix} \tag{12}$$

2.3.2 *Mesoscale Pollutant flows under saturated conditions*

The mass balance equation of the pollutant, under saturated conditions, is:

$$\frac{\partial}{\partial x_i}(v_i^c) = 0 \tag{13}$$

where v_i^c is the pollutant flow rate per unit area [m/s].

The pollutant flows are caused by three phenomenon: advection, dispersion and diffusion. The advection is a movement of the pollutant inside the fluid, due to fluid flows. The dispersion is due to the irregularity of the porous system, causing pollutant concentration to vary locally inside the fluid to accommodate for geometrical constraints. Finally, the diffusion is due to a gradient of concentration of the pollutant inside the fluid itself, and is not caused by a fluid flow. The pollutant flow can therefore be calculated according to the following equation:

$$\begin{aligned} v_i^c &= v_i^{\text{advection}} + v_i^{\text{dispersion}} + v_i^{\text{diffusion}} \\ &= C\, u_i - \cancel{D_{\text{dispersion}} \frac{\partial C}{\partial x_i}} - D_{\text{diffusion}} \frac{\partial C}{\partial x_i} \end{aligned} \tag{14}$$

where the dispersion is neglected, and the diffusion coefficient $D_{\text{diffusion}}$, also noted D, is taken as the diffusion coefficient obtained experimentally.

The contribution of the water flows on the pollutant flows are transmitted through the water velocity u_i, taken equal to:

$$u_i = \frac{v_i^w}{\rho_w} \tag{15}$$

The stiffness matrix is obtained by derivation of the nodal fluxes:

$$K_{LK} = \int_V \nabla N_K D \nabla N_L dV - \int_V N_K \underline{u} \nabla N_L dV \tag{16}$$

2.3.3 *Homogenized macroscale response*

Once the mesoscale fluxes are obtained, they must be homogenized for the macroscale. The fluxes of each integration point are therefore summed up, proportionally to the surface of each integration point.
Once the macroscale has fluxes values for each of its integration point, the forces are computed and the problem is finally solved.

The stiffness matrix of the mesoscale is computed by perturbations: each variable coming from the macroscale (gradient of pressure and mean pressure, gradient of pollutant concentration and mean concentration) are perturbed and the computation is performed at the mesoscale. Then, the results are saved at the macroscale depending on the perturbation applied.

3 RESULTS

The model is fully functional for water flows or diffusion of pollutant. Nonetheless, this paper focuses on the pollutant diffusion only. The results available are therefore:

- Comparison of the multiscale model with a validated macroscale model;
- Comparison of the results for several microstructures: a plain mortar paste, a concrete made from natural aggregates (NAC) and another one from recycled concrete aggregates (RAC);
- Comparison of the results and computation cost for several sizes of RVE.

3.1 *Comparison with a validated macroscale model*

The multiscale model can easily be validated by comparing the results obtained with the results of an already validated macroscale-only model. The applied conditions and the macroscale meshes used are identically the same for both models, and the microscale RVE consist of a plain material with no aggregates, so that the results can be compared.

The macroscale model is composed of a law for pollutant transport inside porous media (Biver 1992) and its 4-noded elements, while our multiscale model is developed for both 4-node and 8-node elements. The comparison is therefore made for the three possible cases: 4 or 8-node multiscale elements, and 4-node macroscale elements. The results are available in the Figure 4.

The applied conditions are the following: the right border has a fixed concentration of 0, while the left border sees an increase of concentration from 0 to 100, varying linearly from 0s. to 86400s., then kept constant until the end of the simulation.
All the models have the exact same response, except for meshing differences between 4-noded and

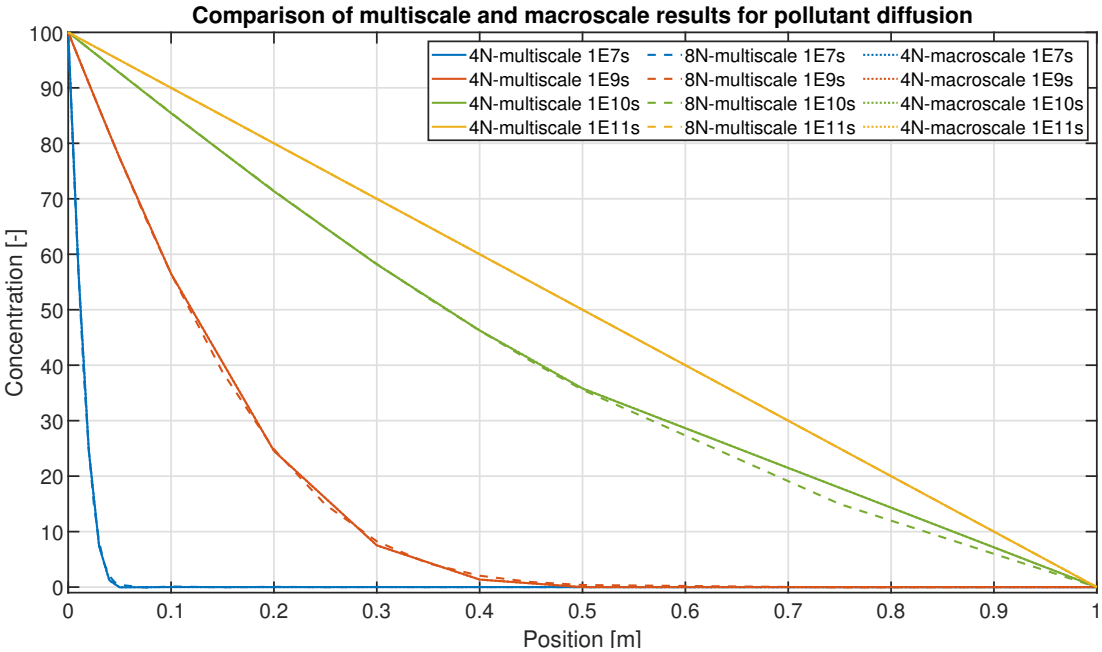

Figure 4: Comparison of the results obtained from a purely 4-node macroscale model and the developed multiscale model (in both 4 and 8-node configurations).

8-noded elements. One can therefore assess that the multiscale model is valid and represents the diffusion of pollutant inside a porous medium accurately.

3.2 *Comparison of several microstructures*

For the first application, a 1D diffusion experiment is modelled for different microstructures. The applied conditions on the left border are the following:

- Pollutant concentration of 0% at 0 seconds;
- Pollutant concentration of 100% at 1E5 seconds, and kept constant until 1E7 seconds. The evolution is linear in between 0 and 1E5 seconds;
- Pollutant concentration of 0% at 1E10 seconds, with a linear decrease too.

The microstructure is modelled by a square RVE of 15mm sides[1]. The NAC and RAC microstructures are exactly the same, except for the adherent mortar paste that can be found around the recycled concrete aggregates and that decrease the size of the impervious aggregates inside.
The new mortar paste has a diffusion coefficient of 1E-12 m^2/s while the adherent mortar paste of the RCA has a diffusion coefficient of 5E-12 m^2/s.

The results are available at Figure 5. The first time represented is at 1E8s., when the concentration is already decreasing at the surface. At that time, the RAC has the greater concentration of the three microstructures, followed by the mortar paste and then the NAC. Once the fluxes start going from inside the material towards the exterior surface, the RAC also displays higher exchange rates than the other microstructures, its concentration being the smallest. This may be surprising as it shows that the small proportion of adherent mortar, whose diffusion coefficient is higher, plays an important role on the diffusion of pollutants. It indeed decreases the total impermeable surface, therefore directly increasing the diffusion capacity of the material. Furthermore, compared to plain mortar paste, the overall diffusion coefficient of the RAC may be higher due to the higher coefficient of the aggregates alone.

Another point worth mentioning is that the two concrete RVE create pollutant fluxes along the y-axis, even though the applied conditions are solely along the x-axis. This is due to the impermeable surfaces that must be by-passed.

3.3 *Computational cost dependency*

The next results concern the influence of the RVE size. Four RVE of 10mm, two times 15mm and 20mm sides have been used, firstly with NAC microstructure and then with RAC. Using two RVE of the same size is useful to observe whether the random disposition and size of the aggregates impact the overall results of the diffusion experiment or not. The two RVEs of 15mm sides are visible on the Figure 6 for the NAC.

[1] A size of 25mm would have been more adequate to respect the $3D_{max}$ rule. However, the computational cost would have been too high for a simple application as this one.

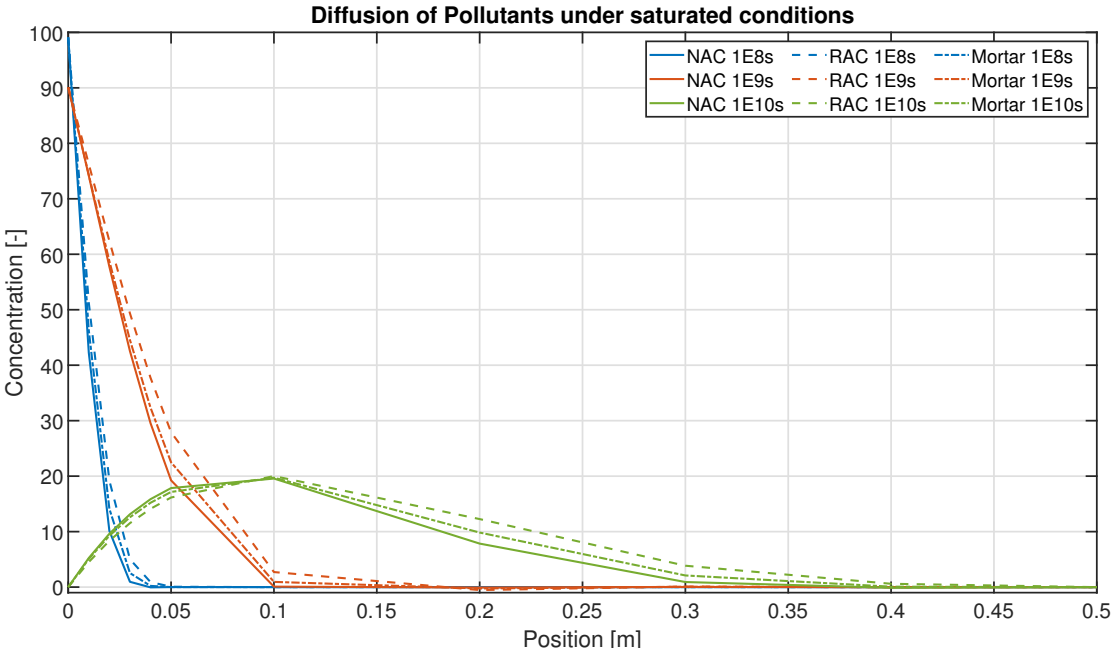

Figure 5: Results obtained for the diffusion of pollutants amongst several types of microstructure: a plain mortar paste, a NAC and a RAC.

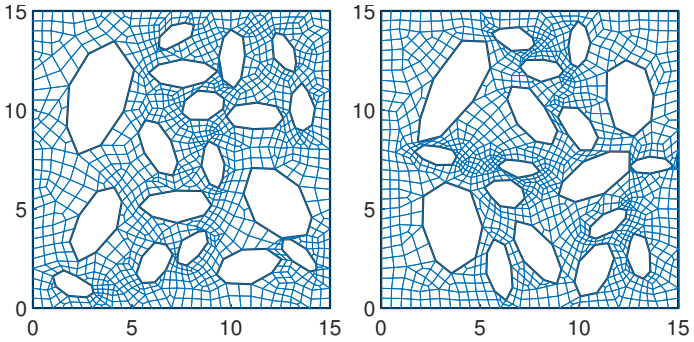

Figure 6: Two RVEs of 15mm side based on the NAC.

Figure 7 represents the evolution of the concentration for the NAC RVE. The first observation is that the two RVE with 15mm side exhibit the same results, which is comforting. Then, one can also observe that the smaller the RVE, the bigger the pollutant fluxes are. This is due to the inability of the RVE generation algorithm to adequately represents the requested granulometric curve when the size of the RVE decreases. There is therefore less aggregates and more mortar paste through which the pollutant can diffuse.
Figure 8 also represents the evolution of the concentration for the same RVE sizes, but for a concrete made from RCA. What is interesting is that the RAC results seem to depend less on the RVE size than the NAC. That may be due to the permeable surface of the RVE being already bigger than for the NAC, leading to fluxes that may not be limited by the permeable surface area but rather by the intrinsic properties of the material.

On Figure 9, representing the computation time with respect to the number of degree of freedom of the RVE, one observes that the computation time is directly linked to both the RVE size and the type of microstructure studied (the RAC is more complex than the NAC and therefore possesses more DOF). Fitting the numerical results with a power equation gives a R-squared value of 0.997 for the following equation:

$$y = 3.46 \times 10^{-12} \times x^{4.793} \tag{17}$$

It is therefore crucial to carefully choose the RVE to be used as it impedes on both the accuracy of the results and the computational time, both being in opposition with each other. In order not to sacrifice one or the other, parallelisation will be necessary.

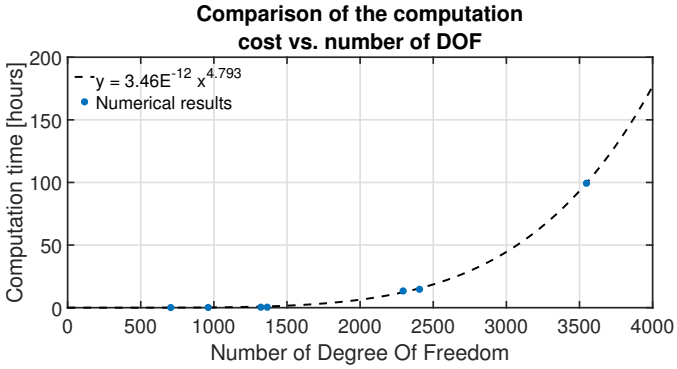

Figure 9: Evolution of the computational cost with respect to the number of Degree of Freedom (DOF) of the problem.

4 CONCLUSION

In conclusion, three observations were made:

1. The multiscale model allows the simulation of a pollutant diffusion inside a porous media, with an accuracy equal to the one of a classical

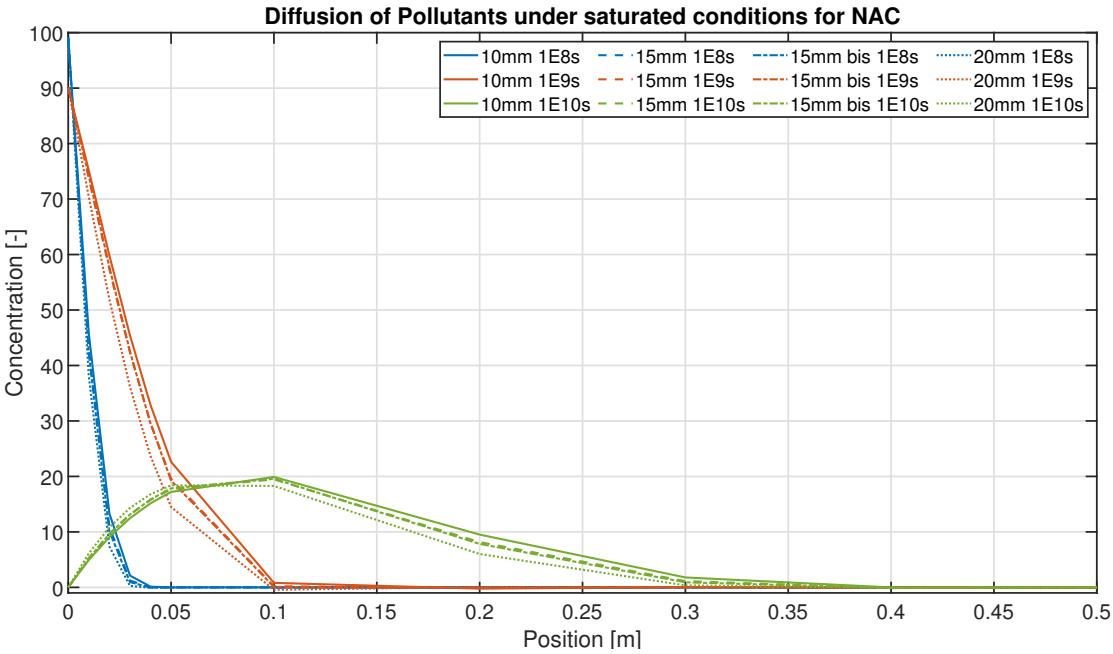

Figure 7: Results obtained for the diffusion of pollutants amongst several sizes of RVE for NAC: 10mm, two times 15mm and 20mm.

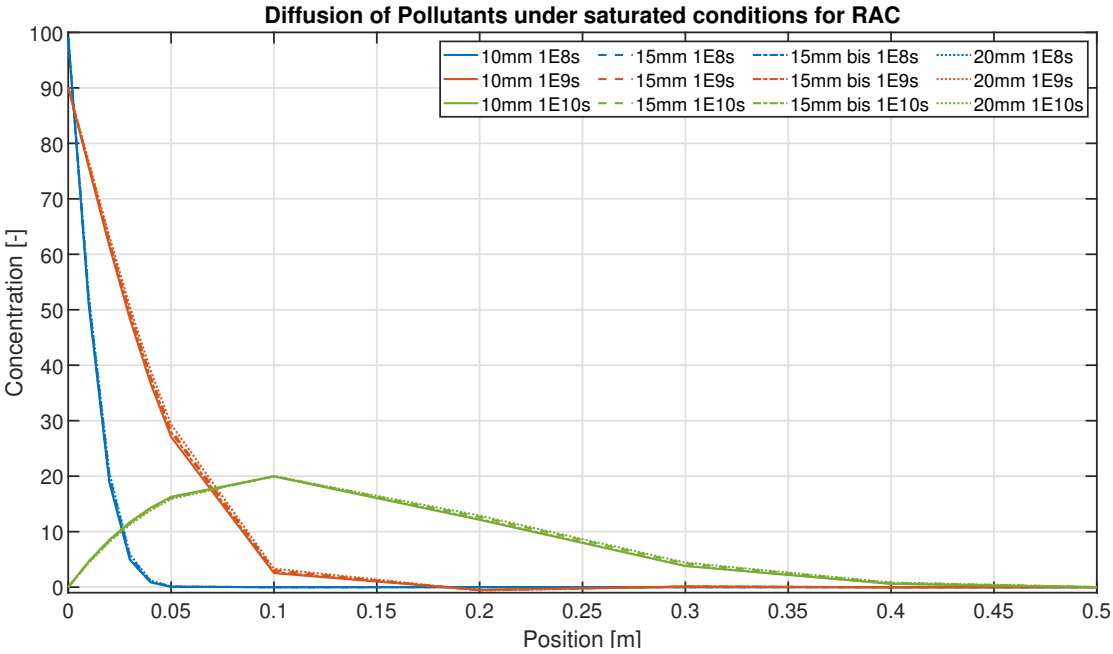

Figure 8: Results obtained for the diffusion of pollutants amongst several sizes of RVE for RAC: 10mm, two times 15mm and 20mm.

simple-scale model. However, it has the advantage of using intrinsic properties instead of homogenized one, possibly depicting results closer to the reality;

2. The model replicates what has been found experimentally: the greater cement content of the RAC allows a greater chloride diffusion than the NAC;

3. The choice of the RVE has a great influence on the results performed; the aggregates add a certain complexity that increases the computation time while also increasing the accuracy of the results for a porous media such as concrete.

ACKNOWLEDGEMENTS

Funding: This work is supported by the Wallonia regional government (Belgium) in the framework of a FRIA (Fund for Industrial and Agricultural Research) grant.

COMPETING INTERESTS

The authors declare that they have no known competing financial interests or personal relationships that could have appeared to influence the work reported in this paper.

REFERENCES

Akbarnezhad, A., K. C. G. Ong., C. T. Tam, & M. H. Zhang (2013, December). Effects of the Parent Concrete Properties and Crushing Procedure on the Properties of Coarse Recycled Concrete Aggregates. *Journal of Materials in Civil Engineering 25*(12), 1795–1802.

Angst, U., B. Elsener, C. K. Larsen, & Ø. Vennesland (2009). Critical chloride content in reinforced concrete - A review. *Cement and Concrete Research 39*, 1122–1138.

Bear, J. & A. Verruijt (1987). *Modeling Groundwater Flow and Pollution*. D. Reidel Publishing Company.

Belin, P., G. Habert, M. Thiery, & N. Roussel (2014, September). Cement paste content and water absorption of recycled concrete coarse aggregates. *Materials and Structures 47*(9), 1451–1465.

Bertrand, F., O. Buzzi, P. Bésuelle, & F. Collin (2020). Hydro-mechanical modelling of multiphase flowin naturally fractured coalbed using a multiscale approach. *Journal of Natural Gas Science and Engineering 78*, 103303.

Biver, P. (1992). *Phenomenal and Numerical study on the propagation of pollutants*. Ph. D. thesis, University of Liège.

European Commission (2019, August). Construction and Demolition Waste (CDW). `https://ec.europa.eu/environment/waste/construction_demolition.htm`. Accessed: 28/08/2020.

Garboczi, E. J. & D. P. Bentz (1998). Multiscale Analytical/Numerical Theory of the Diffusivity of Concrete. *Advanced Cement Based Materials 8*, 77–88.

Geuzaine, C. & J.-F. Remacle (2009). Gmsh: a three-dimensional finite element mesh generator with built-in pre- and post-processing facilities. *International Journal for Numerical Methods in Engineering 79*(11), 1309–1331.

Hu, Z., L. Mao, J. Xia, J. Liu, J. Gao, J. Yang, & Q. Liu (2018). Five-phase modelling for effective diffusion coefficient of chlorides in recycled concrete. *Magazine of Concrete Research 70*(11), 583–594.

Hussain, H., D. Levacher, J.-L. Quenec'h, A. Bennabi, & F. Bouvet (2000). Valorisation des aggrégats issus de bétons de démolition dans la fabrication de nouveaux bétons. *Sciences et techniques 19*, 17–22.

Kouznetsova, V., W. A. M. Brekelmans, & F. P. T. Baaijens (2001). An approach to micro-macro modeling of heterogeneous materials. *Computational Mechanics 27*, 37–48.

Mangat, P. S. & B. T. Molloy (1994). Prediction of long term chloride concentration in concrete. *Materials and Structures 27*, 338–346.

Morga, M. & G. C. Marano (2015, June). Chloride Penetration in Circular Concrete Columns. *International Journal of Concrete Structures and Materials 9*(2), 173–183.

Nagataki, S., A. Gokce, T. Saeki, & M. Hisada (2004). Assessment of recycling process induced damage sensitivity of recycled concrete aggregates. *Cement and Concrete Research 34*, 965–971.

Nilenius, F. (2014). *Moisture and Chloride Transport in Concrete - Mesoscale Modelling and Computational Homogenization*. Ph. D. thesis, Chalmers University of Technology, Gothenburg, Sweden.

Rao, A., K. N. Jha, & S. Misra (2007). Use of aggregates from recycled construction and demolition waste in concrete. *Resources, Conservation and Recycling 50*, 71–87.

Smit, R. J. M., W. A. M. Brekelmans, & H. E. H. Meijer (1998). Prediction of the mechanical behavior of nonlinear heterogeneous systems by multi-level finite element modeling. *Computer Methods in Applied Mechanics and Engineering 155*, 181–192.

Sun, C., Q. Chen, J. Xiao, & W. Liu (2020). Utilization of waste concrete recycling materials in self-compacting concrete. *Resources, Conservation & Recycling 161*, 104930.

Xi, Y. & Z. P. Bazant (1999, February). Modeling Chloride Penetration in Saturated Concrete. *Journal of Materials in Civil Engineering 11*(1), 58–65.

Zhao, Z., L. Courard, S. Groslambert, T. Jehin, A. Léonard, & J. Xiao (2020). Use of recycled concrete aggregates from precast block for the production of new building blocks: An industrial scale study. *Resources, Conservation and Recycling 157*, 104786.